

## SIMULATION OF PARTICLE SEGREGATION IN METALLURGICAL FURNACES FOR IRON PRODUCTION

**Christoph KLOSS<sup>1,5\*</sup>, Philippe SEIL<sup>1</sup>, Franz HAUZENBERGER<sup>3</sup>, Stefan AMBERGER<sup>1</sup>,  
 Christoph FEILMAYR<sup>4</sup>, Stefan PIRKER<sup>1,2</sup>, and Christoph GONIVA<sup>1,5</sup>**

<sup>1</sup> Christian Doppler Laboratory on Particulate Flow Modelling, JKU Linz, AUSTRIA

<sup>2</sup> Institute of Fluid Mechanics and Heat Transfer, JKU Linz, AUSTRIA

<sup>3</sup> Siemens VAI Metals Technologies GmbH, Linz, AUSTRIA

<sup>4</sup> voestalpine Stahl GmbH, Linz, AUSTRIA

<sup>5</sup> DCS Computing GmbH, Linz, AUSTRIA

\*Corresponding author, E-mail address: christoph.kloss@jku.at

### ABSTRACT

Metallurgical processes like the blast furnace or the Siemens Corex® process are widely used for the production of hot metal. Main raw materials include coke and iron ore for the blast furnace process and coal and iron ore for the Corex® process. Typically, these materials are charged into the furnace through chutes, and the process is subsequently subject to particle segregation at different stages of the process: (a) segregation that takes place as the bulk solids are added/charged into the furnace (b) segregation that takes place in the bed, induced by the granular flow pattern (c) segregation induced by gas-solid interaction, e.g. near the so-called raceway (a zone of partial fluidization due to gas injection). Segregation will lead to different segregation patterns and thus different grain size distributions. The grain size distribution is a relevant parameter as it has major influence on the process stability and efficiency by means of pressure drop and homogeneity of the chemical reactions. Numerical Discrete Element Method (DEM) simulations were performed to show that different ways of adding the granular material into the vessel ('charging recipes') lead to different segregation patterns and grain size distributions.

### NOMENCLATURE

#### Greek Symbols

$\alpha$  volume fraction [1]  
 $\delta$  particle-particle overlap [m]  
 $\mu$  dynamic viscosity [kg/(m s)]  
 $\nu$  kinematic viscosity [Pa s]  
 $\mu_c$  Coulomb friction coefficient [1]  
 $\rho$  density [kg / m<sup>3</sup>]  
 $\tau$  stress tensor [Pa]  
 $\omega$  rotational velocity [1/s]

#### Latin Symbols

A particle-particle contact area [m<sup>2</sup>]  
 c damping coefficient [kg/s]  
 C<sub>d</sub> drag coefficient [1]

d (particle) diameter [m]  
 D hopper orifice diameter [m]  
**F** force [N]  
**g** gravity constant [m/s<sup>2</sup>]  
 I moment of inertia [kg m<sup>2</sup>]  
 k stiffness [N/m]  
**K** momentum exchange coefficient [ks / (s m<sup>2</sup>)]  
 m mass [kg]  
 •  
*m* mass flow-rate [kg/s]  
 p pressure [Pa]  
 r radius [m]  
 R<sub>μ</sub> rolling friction coefficient [1]  
**u** velocity [m/s]  
 $\Delta \mathbf{u}$  relative velocity [m/s]  
 t time [s]  
 $\Delta t$  time-step size [s]  
**T** torque [Nm]  
 V volume [m<sup>3</sup>]  
**x** position [m]  
 $\Delta \mathbf{x}$  particle overlap at contact point [m]

#### Sub/superscripts

1 left hopper  
 2 right hopper  
 c contact  
 d drag  
 f fluid  
 i particle index  
 n normal to contact point  
 p particle  
 r rolling friction  
 s solid  
 t tangential to contact point

### INTRODUCTION AND OUTLINE

Size segregation in counter-current aggregate like a blast furnace or the melter-gasifier of the Corex® process is affecting the radial distribution of the charged burden and thus influencing the distribution of gas in the shaft and cohesive zone. Predicting and controlling this segregation

is crucial to the efficiency of the process. Furthermore, a smooth burden descent is desired to achieve undisturbed gas flow. Given the harsh environment that these processes operate under, lab-scale experimental methods as well as analytical and numerical methods are valuable tools to gain insight into the physics of the process. Lab-scale experiments have been performed e.g. by Wright et al, 2011, and analytical approaches e.g. by Dong et al (2007) and Ueda et al (2010).

On the numerical side, Discrete Element Method (DEM) modelling gains more and more popularity in the scientific community (e.g. Zhou, 2008; Mio, 2012).

In this paper, we want to present an overview over all the steps necessary to simulated burden flow using the Discrete Element Method: Validation, Calibration and Application. Therefore, the paper is structured as follows: First, an overview over modelling strategy will be provided. Then, lab-scale validation results are presented and the necessity of calibrating model parameters to correctly mimic the behaviour of the granular material is highlighted. Finally, we present results of the process-scale simulations.

## MODEL DESCRIPTION

### Discrete Element Method

The Discrete Element Method (DEM) was introduced by Cundall and Strack (1979). In the frame of the DEM, all particles in the computational domain are tracked in a Lagrangian way, explicitly solving each particle's trajectory, based on the force and torque balances:

$$m_p \ddot{\mathbf{x}}_p = \mathbf{F}_{p,n} + \mathbf{F}_{p,t} + \mathbf{F}_{p,f} + \mathbf{F}_{p,b} + \mathbf{F}_{p,p} + \mathbf{F}_{p,v} \quad (1)$$

$$\mathbf{I}_p \frac{d\boldsymbol{\omega}_p}{dt} = \mathbf{r}_c \times \mathbf{F}_{p,t} + \mathbf{T}_{p,r} \quad (2)$$

where  $\mathbf{F}_{p,n}$  and  $\mathbf{F}_{p,t}$  are the normal and tangential particle-particle contact force.  $\mathbf{F}_{p,p}$  is the force due to fluid pressure acting on the particle surface, which can be split up into the force due to buoyancy and the pressure gradient force, which is based on the piezometric pressure  $P_{\text{rgh}} = p - \rho_f \mathbf{g} \cdot \mathbf{x}$ , where  $\rho_f$  denotes the fluid density,  $\mathbf{g}$  the gravitational acceleration and  $\mathbf{x}$  the coordinate vector.  $\mathbf{F}_{p,v}$  is the viscous fluid force acting on the grain.  $\mathbf{F}_{p,f}$  is the drag force that the fluid and particle phase exchange. Other body forces like gravity, electrostatic or magnetic forces are summarized to  $\mathbf{F}_{p,b}$ .

Each physical particle is mathematically represented by a specified geometric shape, e.g. a sphere (see Figure 1). The translational and angular accelerations of a particle are based on the corresponding momentum balances. Using a soft-sphere approach, the particles are allowed to overlap slightly. The normal force tending to repulse the particles can then be calculated from this spatial overlap  $\Delta \mathbf{x}_p$  and the normal relative velocity at the contact point,  $\Delta \mathbf{u}_{p,n}$ . For further information the reader is referred to Pöschel and Schwager (2005). The above mentioned forces and torques are summarized in Table 1. Terms  $\mathbf{F}_{p,p}$ ,  $\mathbf{F}_{p,v}$ ,  $\mathbf{F}_{p,f}$  are terms stemming from a surrounding fluid and are thus evaluated in the frame of CFD-DEM approach (Tsuji et al. (1993); Zhu et al. (2007, 2008) and Zhou et al. (2010)). In the frame of this study, these terms are

neglected. For more details on  $\mathbf{F}_{p,p}$ ,  $\mathbf{F}_{p,v}$ , and  $\mathbf{F}_{p,f}$  please refer to Goniva (2012a).

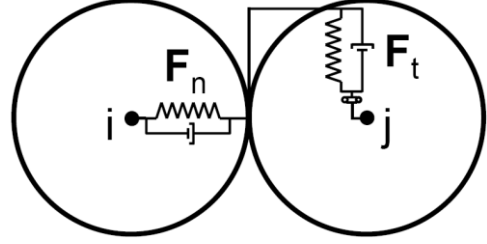


Figure 1: DEM spring-dashpot model.

$$\mathbf{F}_{p,n} = -k_n \Delta \mathbf{x}_p + c_n \Delta \mathbf{u}_{p,n}$$

$$\mathbf{F}_{p,t} = \min \left\{ \left| k_t \int_{t_{c,0}}^t \Delta \mathbf{u}_{p,t} dt + c_t \Delta \mathbf{u}_{p,t} \right|, \mu_c F_{p,n} \right\}$$

$$\mathbf{F}_{p,b} = \mathbf{g} m_p$$

$$\mathbf{T}_{p,r} = R_\mu k_n \Delta \mathbf{x}_p \frac{|\boldsymbol{\omega}_{\text{rel}}|}{|\boldsymbol{\omega}_{\text{rel}}|} \frac{d}{2}$$

Table 1: Modelling conditions.

### Overall Simulation approach

In the frame of this study we focused on the granular flow only. The influence of the gas phase and the liquid phases in the furnace (hot metal and slag) was neglected, but is planned for further studies

From a physical point of view, the charging phase and the bed build-up phase exhibit different granular flow regimes (e.g. Rao and Nott, 2008). While the rapid distortion regime prevails in the charging phase, slow granular flow is encountered in the bed region. Furthermore, these two processes can be de-coupled from each other, i.e. the result of the charging process can be seen as input for the flow in the bed. Subsequently, the modelling approach was chosen as follows (see Figure 2):

1. Particles are charged into the furnace from the top using a rotating chute (e.g. a Gimbal®). This process is pictured by a DEM simulation which delivers a spatial impingement distribution and corresponding impingement velocity statistics (**Phase I**).
2. These spatial impingement distribution and velocity statistics serve as inlet for the simulation of the whole bed (**Phase II**).

For **phase I**, the diameter distribution of the granular material is pictured in 1:1 scale. In real operation, the chute rotates, but the forces stemming from rotation are negligible. Thus, in the phase I simulation, this rotation of the chute is not simulated – rather the spatial impingement and velocity statistics are rotated to gather the statistics as they would be found in the real process.

In the **phase II** simulation, a slice of the furnace (e.g. a melter-gasifier of the Corex® process) is simulated. Based on the geometry on the process, assumptions about the locations of the so-called ‘raceway’ (region where combustion takes place) and the ‘cohesive zone’ (where the Fe-carrier begins to melt) are made (see Figure 2). As

the global mass-flow rates for the process are known, sinks for the C-carrier (e.g. coke or coal) are defined in the raceway zone, and sinks for the Fe-carrier are defined in the cohesive zone. Furthermore, there is the possibility to change the material parameters for the particles as they enter the cohesive zone, thereby picturing the increased stickiness.

It is important to note that it is currently impossible to picture the real number of particles present in such a large industrial vessel. Thus, a strategy to enlarge the particles while preserving (termed “coarse graining”) is used. In this work, the coarse graining approach presented by Bierwisch (2009) is used. Secondly, as long time scales have to be simulated (in our case ~14 hours), a “temporal speed-up” of the mass flow-rate is used, which is feasible to a certain degree (Rycroft, 2007). For further simulation speed-up, MPI-based load-balancing is used to improve the spatial load distribution among the processes. Following the approach presented by Kloss et. al. (2011a, 2011b) and Kloss (2011c), the axis-parallel process-boundaries are dynamically re-computed during the simulation. This procedure is sketched in Figure 3.

The simulation codes that have been used are LIGGGHTS (2012) for the DEM simulation and CFDEMcoupling (2012) for the particle volume fraction evaluation. Both codes are distributed under open source license by the authors of this paper.

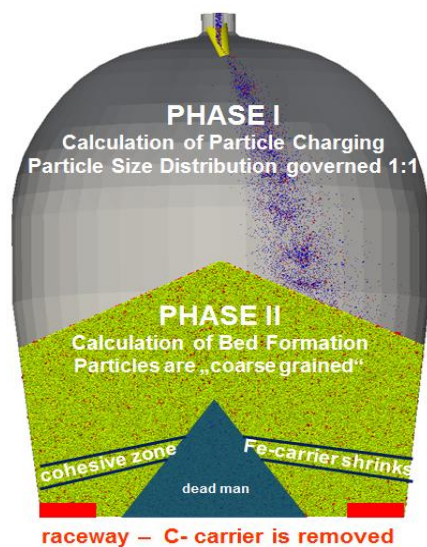


**Figure 2:** Simulation approach sketched for a melter gasified of the Corex® process.

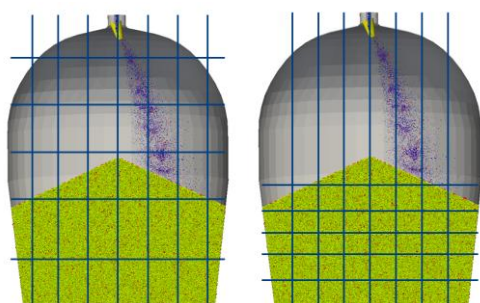


**Figure 3:** Sketch MPI-based load-balancing approach. Non-balanced configuration (left) and load-balanced configuration (right).

## VALIDATION OF SIMULATION APPROACH

Ensuring the validity of the simulation approach is a crucial part of numerical modelling. On a first (more software-engineering related) level, software quality control is applied to our simulation code (Amberger et al, 2011) to ensure long-term consistency of the simulation results as good as possible.

Secondly, validation of the concrete simulation model/approach should be performed. As outlined earlier, the simulation approach is divided into two phases exhibiting different physical regimes (rapid distortion regime and slow granular flow regime), so we have structured our lab- scale validation into two phases as well:

1. In **validation phase I**, a lab-scale charging experiment with glass beads was conducted.
2. In **validation phase II**, lab-scale experiments where both the charging phenomenon and the bed build-up were included.

Experimental set-up and simulation results for validation phase I were published by Kloss et. al. (2009). Simulation and experiments showed a good agreement.

The experimental rig designed for validation phase II is depicted in Figure 4. The setup consists of a main body and a box, both made of Perspex. In addition, two hoppers are placed on top of the facility. The main body of the setup has two chutes of 45°, which divert the particles into a free-fall section. In the lower part, a removable box divided into twelve compartments is inserted, each of which has a stamp which can be moved up and down. By lowering the bed into the box compartments a fractional segregation analysis can be performed. The numbering convention to identify the compartments is also shown in Figure 4.

Each hopper was filled with 9 kg of glass beads of different diameter, and 3 different cases with respect to hopper mass flow-rate and particle diameter were focused in both simulation and experiment, which are shown in Figure 5. For the simulations, the discharging of the hoppers was not simulated directly. The discharge rate was rather determined experimentally and instead of resolving the outflow of the hoppers, particles were inserted to match the measured mass flow rate. For these three cases shown in Figure 5, the mass fraction distributions in the twelve compartments obtained experimentally and numerically are shown in Figure 6 - Figure 8. Cases A and B show a very good agreement, and in case C, qualitative agreement can be found.

Further details on the validation phase II experiments have been published by Ortega-Goméz (2010). For details on numerical results, discussion of the results and a detailed segregation analysis the reader is referred to the work of Seil (2012).

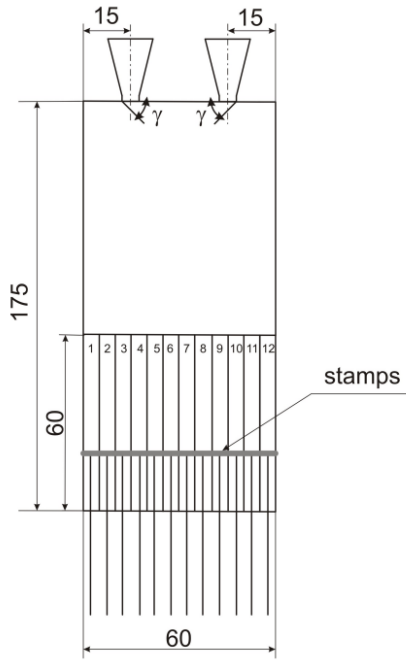


**Figure 4:** Schematic of geometry for phase II lab-scale validation (lengths in cm), from Ortega-Goméz (2010)

Case	$d_1$ (mm)	$d_2$ (mm)	$D_1$ (mm)	$D_2$ (mm)	$\dot{m}_1$ (kg/s)	$\dot{m}_2$ (kg/s)
A	4	3.15	38	34	0.66	0.506
B	4	3.15	38	22	0.66	0.113
C	6	2.65	38	34	0.573	0.539

**Figure 5:** Cases for phase II lab-scale validation, from Seil (2012). Subscripts “1” and “2” denote the left and right hopper in Figure 4, respectively.

### MODEL CALIBRATION

After validating the simulation approach on the lab-scale, we have to ensure that the model approach is also valid for the material that is used in the industrial process to be simulated. As there is no direct link between DEM model parameters and parameters of the bulk material, this step involves calibration of the model parameters. Calibration tests may comprise e.g. angle of repose experiments, friction tests and shear cell experiments. As an example, Figure 9 and Figure 10 show simple angle of repose tests with sinter and pellet particles, which are typical raw materials for the blast furnace process. This information can then be used to calibrate the DEM parameters so that the angle of repose is pictured (Figure 11). The main influence parameter on the angle of repose is given by the rolling friction coefficient  $R_\mu$  (see Table 1). Instead of using a rolling friction model, one can approximate the shape of the particles directly. This can be realized by polyhedral particle surfaces (Pöschel and Schwager, 2005; Höhner et al, 2011), super-quadric shapes (Cleary and Sinnott, 2008) or the multi-sphere approach (Krugger-Emden, 2009; Höhner et al, 2011). The left picture in Figure 12 shows a CAD model of a sinter particle which was obtained from a laser scan of the particle. This CAD data can then be used to generate a shape approximation, e.g. by clumps of spheres (center picture in Figure 12). Detailed information about this procedure can be found in Amberger (2012).

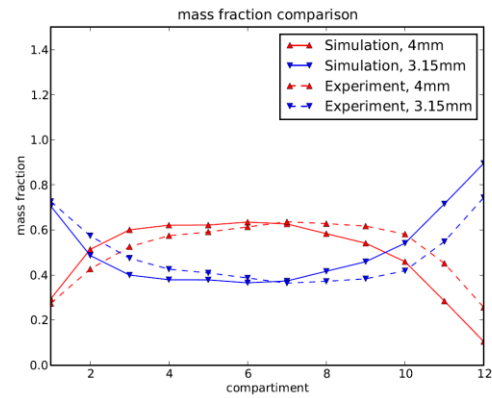


**Figure 6:** Mass fraction per compartment for case A of phase II lab-scale validation, from Seil (2012).

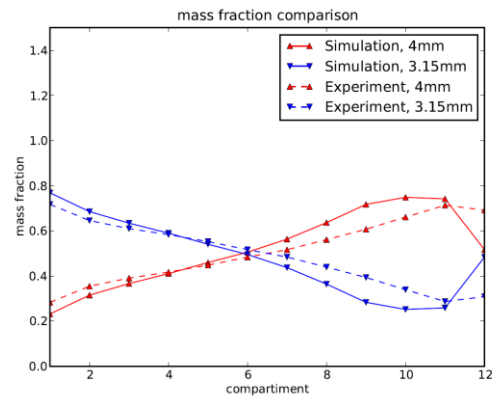


**Figure 7:** Mass fraction per compartment for case B of phase II lab-scale validation, from Seil (2012).

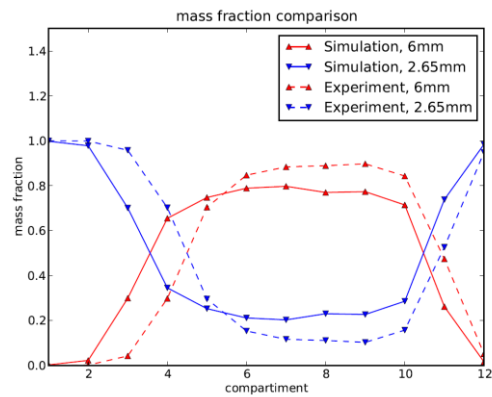


**Figure 8:** Mass fraction per compartment for case C of phase II lab-scale validation, from Seil (2012).

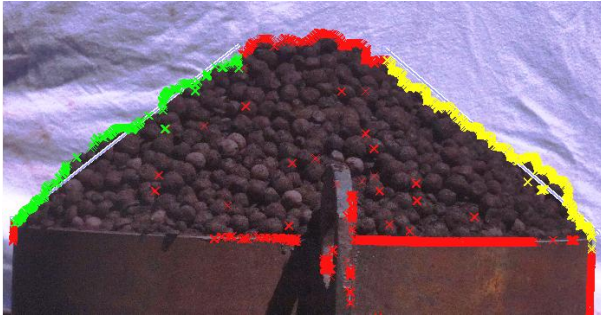


**Figure 9:** Angle of repose test for pellets with shape recognition by image processing, with an angle of repose of  $\sim 37^\circ$ .

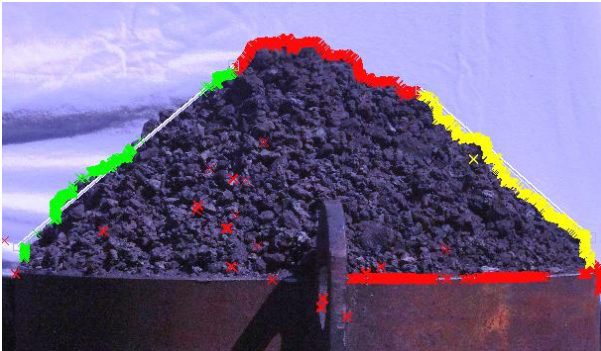


**Figure 10:** Angle of repose test for sinter with shape recognition by image processing, with an angle of repose of  $\sim 40^\circ$ .

### PROCESS SCALE SIMULATION

After the model calibration phase, a set of different cases were simulated for a Corex® melter gasifier. In the frame of this paper, 2 cases are focused:

- (A) **Central charging**, where the material is added to the centre of the furnace, and
- (B) **Boundary charging**, where all the material is added at the boundary of the furnace.

In typical operation, such a furnace is operated using a charging recipe that varies dynamically between those two extreme cases. As outlined above, particle charging was simulated in a first step to gather spatial impingement and velocity statistics for the bed simulations, which are presented in this section. Simulations of the bed comprised  $\sim 150,000$  spherical particles and were performed with a time-step of  $\Delta t = 1e-5$  sec, a coarse-graining ratio of 8, and a temporal speed-up of 250. Simulations were run for 20,000,000 time-steps, so that including the temporal speed-up a real time of 13.8 hours of operation were simulated. Run-time was 12 days on 12 processors using the load-balancing approach sketched in Figure 3. Snapshots of the simulation results are shown in Figure 13-Figure 17. The velocity plot in Figure 13 shows the so-called ‘dead-man’, a stable region of stationary char particles in the centre of the furnace. In Figure 16, no stable dead man establishes. It can be seen in Figure 14 and Figure 17 that the central charging and boundary charging cases lead to different segregation patterns: For central charging, large particles accumulate near the wall, and for boundary charging, large particles accumulate at the centre of the vessel.

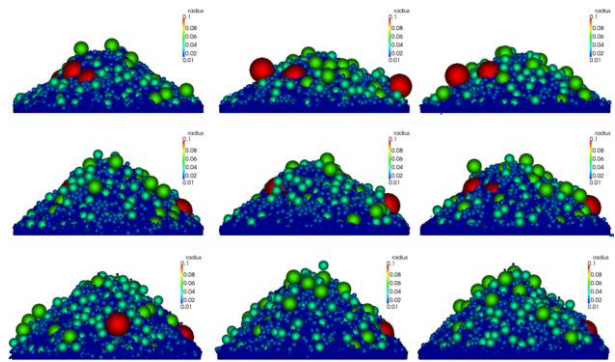


**Figure 11:** Calibration of DEM model with angle of repose experiment. The three vertical columns correspond to coefficient of friction values of 0.5, 0.7 and 0.9, respectively. The three horizontal rows correspond to coefficient of rolling friction values of 0.07, 0.14 and 0.21, respectively. The angle of repose varies from  $\sim 33^\circ$  (upper left) to  $\sim 43^\circ$  (lower right).

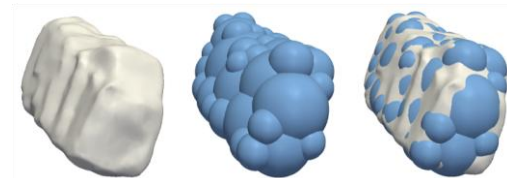


**Figure 12:** Laser scan of a sinter particle (left), multi-sphere approximation of this particle (centre) and visualization of shape accuracy and off-volume (right). Taken from Amberger (2012).

It is known that particles forming a heap will tend to segregation where large particles roll down the slope, whereas small particles will tend to percolate. The segregation pattern will have implications for the gas-flow, due to changed flow resistance. Figure 15 shows a snap shot of the fluid volume fraction (or void fraction) field  $\alpha_f$  which has direct impact on the pressure drop and homogeneity of the chemical reactions. It can be seen that the inhomogeneity in the grain size distribution are reflected in the void fraction field.

### CONCLUSION AND OUTLOOK

A numerical study on particle segregation in furnaces for hot metal production was presented. Simulation approach, lab-scale experimental validation and parameter calibration was highlighted. Plant-scale simulations of a Siemens Corex® melter gasifier showed how different recipes of adding the granular material (‘charging recipes’) impact on the grain size distribution and void fraction field, which are directly linked to important process parameters like pressure drop and homogeneity of the chemical reactions. Thus, this DEM simulation technique can be used to develop optimized charging recipes for optimizing process efficiency or for improving product quality. However, future studies should also include full coupling to the gas phase and potentially a liquid phase (hot metal/slag). Also, industrial-scale validation experiments will be focused.

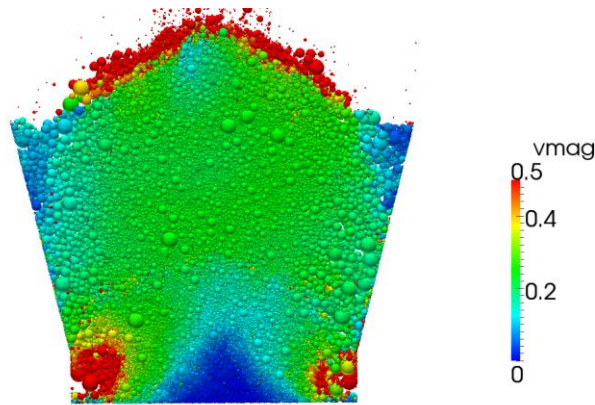


**Figure 13:** Process Scale Simulation – Case A: Central charging: simulation snap-shot of grain velocity distribution

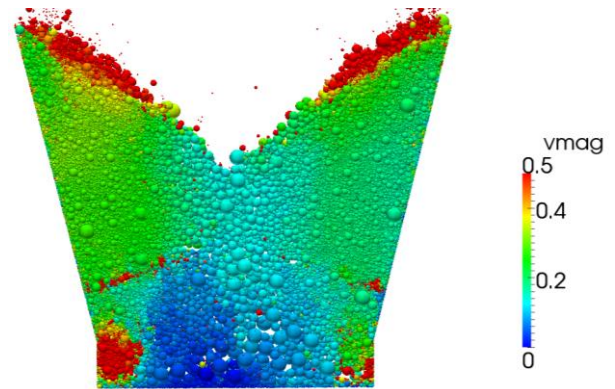


**Figure 16:** Process Scale Simulation – Case B: Boundary charging: simulation snap-shot of grain velocity distribution

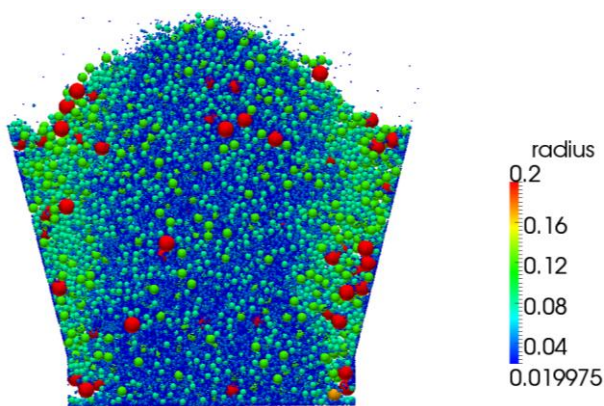


**Figure 14:** Process Scale Simulation – Case A: Central charging: simulation snap-shot of grain size distribution.

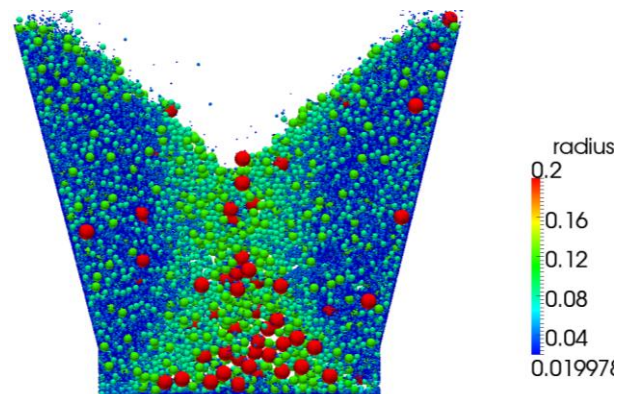


**Figure 17:** Process Scale Simulation – Case B: Boundary charging: simulation snap-shot of grain size distribution.

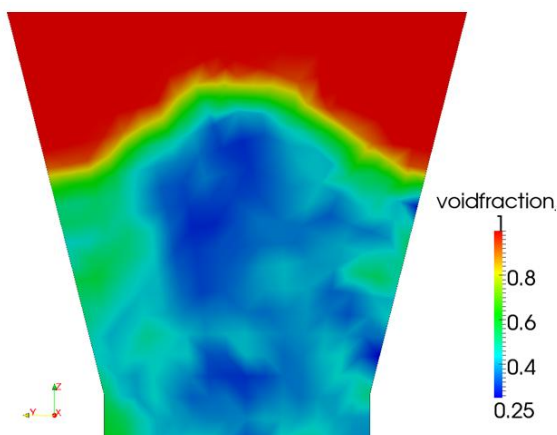


**Figure 15:** Process Scale Simulation – Case A: Central charging: simulation snap-shot of fluid volume fraction ( $\alpha_f$ ) distribution.

## ACKNOWLEDGEMENTS

The authors gratefully acknowledge the funding provided by the Christian Doppler Research Association, the Austrian Ministry of Economy, and the Austrian National Foundation for Research, Technology and Development. The authors also thank Florian Aigner and Michael Friedl (both JKU) for performing the angle of repose experiments and the laser scanning experiments, respectively.

## REFERENCES

- AMBERGER, S., GONIVA, C., HAGER, A., KLOSS, C. (2011): “Strategies for Simulation Software Quality Assurance applied to Open Source DEM”, *Proc. II International Conference on Particle-based Methods - Fundamentals and Applications (PARTICLES 2011)*, Barcelona
- AMBERGER, S., FRIEDL, M., GONIVA, C., PIRKER, S., & KLOSS, C. (2012): “Approximation of objects by spheres for multisphere simulations in DEM”, *Proc. European Congress on Computational Methods in Applied Sciences and Engineering (ECCOMAS 2012)*, Vienna, Austria
- BIERWISCH, C., KRAFT, T., RIEDEL, H., MOSELER, M. (2009): “Three-dimensional discrete element models for the granular statics and dynamics of powders in cavity filling”, *Journal of the Mechanics and Physics of Solids*, **57(1)**, 10–31

- CUNDALL, P.A. STRACK, O.D. (1979): "A discrete numerical model for granular assemblies", *Geotechnique*, **21**, 47-65.
- CFDEMcoupling (2012). "CFD-DEM coupling." Retrieved July 6th, 2012, from <http://www.cfdem.com>
- CLEARY, P.W. SINNOTT, M.D. (2008): "Assessing mixing characteristics of particle-mixing and granulation devices", *Particuology*, **6** (6), December 2008, Pages 419-444
- X.F. Dong, A.B. Yu, J.I. Yagi, P. Zulli (2007): Modelling of multiphase flow in a blast furnace: recent developments and future work, *ISIJ Int.*, **47** (2007), pp. 1553-1570
- GONIVA, C., KLOSS, C., HAGER, A. and PIRKER, S., (2010), "An Open Source CFD-DEM Perspective.", *Proc. of OpenFOAM Workshop, Göteborg, Sweden*, June 22.-24.
- GONIVA, C., KLOSS, C., HAGER, A. WIERINK, G., & PIRKER, S., (2011), „A Multi-Purpose CFD-DEM Approach.", *Proc. 8th International Conference on CFD in Oil & Gas, Metallurgical and Process Industries, SINTEF/NTNU, Trondheim, Norway*
- GONIVA, C., KLOSS, C., DEEN, N.G., KUIPERS, J.A.M., and PIRKER, S., (2012a), "Influence of rolling friction on single spout fluidized bed simulation", *Particuology*, in press
- GONIVA, C., GRUBER, K. and KLOSS, C., (2012b), "Sediment Erosion a Numerical and Experimental study", *Proc. of Riverflow Conference, San José, Costa Rica*, September 5.-7.
- HÖHNER, D., WIRTZ, S., KRUGGEL-EMDEN, H., SCHERER, V. (2011): "Comparison of the multi-sphere and polyhedral approach to simulate non-spherical particles within the discrete element method: Influence on temporal force evolution for multiple contacts", *Powder Technology*, **208**(3), 643-656
- PÖSCHEL, T., SCHWAGER, T. (2005): *Computational Granular Dynamics*, Springer
- Koch, D.L., Hill, R. J. (2001): "Inertial effects in suspension and porous-media flows". *Annual Review of Fluid Mechanics*, **33**, 619.
- KLOSS, C., HERRAN-ONTOSO, L., AICHINGER, G. and PIRKER, S. (2009): „ACCELERATING COUPLED DEM-CFD SIMULATIONS", *Proc. International Conference on Particle-Based Methods*, Barcelona
- KLOSS, C., GONIVA, C., & PIRKER, S., (2010a), "Open source DEM and CFD-DEM with LIGGGHTS and OpenFOAM®", *Proceedings of Open Source CFD International Conference*, Munich, Germany.
- KLOSS, C., GONIVA, C., KLOSS (2010b), "LIGGGHTS – A New Open Source DEM Simulation Software", *Proc. 5th Intl. Conf. on Discrete Element Methods*, London, August 25-26.
- KLOSS, C., GONIVA, C., PIRKER, S., (2011a): "Open Source DEM with LIGGGHTS: Code Overview and Parallel Scalability", *II International Conference on Particle-based Methods - Fundamentals and Applications (PARTICLES 2011)*, Barcelona, October 2011
- KLOSS, C., GONIVA, C., AMBERGER, S., & PIRKER, S., (2011b), „LIGGGHTS Open Source DEM: Models, Features, Parallelism and Quality Assurance", *Proc. 8th International Conference on CFD in Oil & Gas, Metallurgical and Process Industries, SINTEF/NTNU, Trondheim, Norway*
- KLOSS, C. (2011c): "Enhancing LAMMPS Capabilities: Granular Models, Coding Concepts, CAD Interoperability and Coupling to Continuum Methods", Keynote at the 2<sup>nd</sup> LAMMPS workshop, Albuquerque, US, August 9-11, Retrieved Jul 6<sup>th</sup>, 2012
- KLOSS, C., GONIVA, C., HAGER, A., AMBERGER, S., & PIRKER, S., (2012): "Models, algorithms and validation for opensource DEM and CFD-DEM", *J. Progress in Computational Fluid Dynamics*, **2**(3), 140-152
- KRUGGEL-EMDEN, H., RICKELT, S., WIRTZ, S., SCHERER, V. (2008); "A study on the validity of the multi-sphere Discrete Element Method", *Powder Technology*, **188**(2), 153-165
- LAMMPS (2012). *LAMMPS user manual*, Sandia National Laboratories, USA. Retrieved July 6th, 2012, from <http://lammps.sandia.gov/doc/Manual.html>
- LIGGGHTS (2012). "LAMMPS improved for general granular and granular heat transfer simulations." Retrieved July 6th, 2012, from <http://www.liggghts.com>
- MIO, H., KADOWAKI, M., MATSUZAKI, S., KUNITOMO, K. (2012): "Development of particle flow simulator in charging process of blast furnace by discrete element method", *Minerals Engineering*, **33**, 27-33
- OpenCFD Ltd. (2012), "OpenFOAM — The open source CFD toolbox." Retrieved July 6th, 2012, from <http://www.openfoam.com>
- ORTEGA GÓMEZ, J. (2010): *Granular Experiments on Hopper Flow, Particle Charging and Bed Formation*, MSc thesis, JKU Linz
- RAO, K., NOTT, P. (2008): *An introduction to Granular Flow*, Cambridge Series in Chemical Engineering, Cambridge.
- RYCROFT (2007). *Multiscale Modeling in Granular Flow*, PhD thesis, Massachusetts Institute of Technology
- SEIL, P. ORTEGA-GOMEZ, J., PIRKER, S., & KLOSS, C. (2012): "Numerical and experimental study on segregation patterns in granular flow from two hoppers", submitted for *Proc. European Congress on Computational Methods in Applied Sciences and Engineering (ECCOMAS 2012)*, Vienna, Austria, September 10-14,
- TSUJI, Y., KAWAGUCHI, T. and TANAKA, T. 1993. "Discrete particle simulation of two-dimensional fluidized bed", *Powder Technology* **77**, 79-87.
- UEDA, S., NATSUI, S., NOGAMI, H., YAGI, J., ARIMAYA, T. (2010): "Recent Progress and Future Perspective on Mathematical Modeling of Blast Furnace" *ISIJ Int.*, **50**, 914-923
- WRIGHT, B., ZULLI, P., ZHOU, Z.Y., YU A.B. (2011): "Gas-solid flow in an ironmaking blast furnace — I: Physical modelling", *Powder Technology*, **208**(1), 86-97
- ZHU, H.P., ZHOU, Z.Y and YANG, R.Y., YU A.B. (2007): "Discrete particle simulation of particulate systems: Theoretical developments". *Chemical Engineering Science*, **62**(13), 378-396.
- ZHU, H.P., ZHOU, Z.Y and YANG, R.Y., YU A.B. (2008). "Discrete particle simulation of particulate systems: A review of major applications and findings". *Chemical Engineering Science*, **63**, 5728-5770.
- Z.Y. ZHOU, H.P. ZHU, B. Wright, b, A.B. Yu, , , P. Zulli (2011): "Gas-solid flow in an ironmaking blast furnace - II: Discrete particle simulation, *Powder Technology*, **208**(1) , 72-85
- ZHOU, Z. Y.; KUANG, S. B.; CHU, K. W.; YU, A. B. (2010). "Discrete particle simulation of particle-fluid flow: model for-mulations and their applicability", *Journal of Fluid Mechanics*, **661**, 482-51